

Should You Go Deeper? Optimizing Convolutional Neural Network Architectures without Training by Receptive Field Analysis

Mats L. Richter
Osnabrück University
Osnabrueck, Germany

Email: matrichter@uni-osnabrueck.de

Julius Schöning
Osnabrück University of Applied Sciences
Osnabrueck, Germany

Email: j.schoening@hs-osnabrueck.de

Ulf Krumnack
Osnabrück University
Osnabrueck, Germany

Email: krumnack@uni-osnabrueck.de

Abstract—Applying artificial neural networks (ANN) to specific tasks, researchers, programmers, and other specialists usually overshoot the number of convolutional layers in their designs. By implication, these ANNs hold too many parameters, which needed unnecessarily trained without impacting the result. The features, a convolutional layer can process, are strictly limited by its receptive field. By layer-wise analyzing the expansion of the receptive fields, we can reliably predict sequences of layers that will not contribute qualitatively to the inference in the given ANN architecture. Based on these analyses, we propose design strategies to resolve these inefficiencies, optimizing the explainability and the computational performance of ANNs. Since neither the strategies nor the analysis requires training of the actual model, these insights allow for a very efficient design process of ANNs architectures which might be automated in the future.

Index Terms—receptive fields, optimizing, design process, explainability

I. INTRODUCTION

The design of convolutional neural network (CNN) classifier architectures is a process founded firmly in comparative evaluation [1], [2]. Highly aggregated performance metrics like accuracy, model complexity, and computation efficiency are the current basis for comparing different architecture variants to conclude the effect of design decisions. In these metrics, the model complexity is simplified by the number of trainable parameters and the computation efficiency is expressed by the floating-point operations per second (FLOPs) required per forward-pass computation. For designing ANN architectures, these metrics are commonly used. Thus, the design process of ANN is quite explorative following the trial-and-error method. Beyond that is the creation of these metrics for all architectures quite resource-intensive and unsustainable. For a more efficient design process, analysis methods are required allowing conscious design decisions. Ideally, these new design processes work without the training of the ANN for several epochs and can express the efficiencies of each CNN layer.

Reflecting the current design process or design strategy; the number of trainable parameters of the CNN architectures is simply increased, gaining higher accuracy in terms of predictive performance. The continuing trend of this strategy,

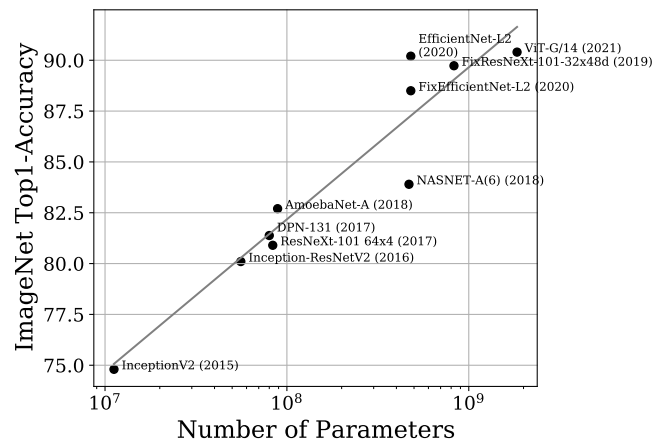


Fig. 1. Selected state-of-the-art ANN architectures from recent years show that improvements in predictive performance strongly coincide with increased trainable parameters and computation complexity. Despite some outliers, like EfficientNet, there is a trend of developing more accurate architectures by just increasing the trainable parameters.

is illustrated in Fig. 1. However, the increase of trainable parameters is generally related to increased computational complexity and increased input data required for training the ANN. These coherences limit the ability to develop, train, and deploy these ANN architectures efficiently and sustainably without wasting energy for unnecessary computations. Making the design of CNN more accessible and enable researches to design beneficial architectures, a design process without training every new architecture is required. In the following, an alternative, efficiency-oriented design paradigm based on the receptive field analysis is introduced.

The receptive field of a unit in a convolutional layer is the area on the input image that influences the output of the unit. Since convolutional layers can be considered pattern detectors, the receptive field is thus the natural upper limit to the size of patterns that a unit in a convolutional layer can detect. Since each convolutional layer operates on the output map of its predecessor, mapping multiple positions of that input into a single position on its output feature map, the receptive field effectively expands in the sequence of

convolutional layers. This progressive growth of the receptive field in a convolutional neural network allows for the detection of increasingly larger patterns in deeper layers. In essence, the growth of the receptive field inside a convolutional neural network controls which layers are capable of fully processing certain features. We [3] show that this can lead to mismatches between neural architecture and input resolution, causing a loss of efficiency and predictive performance, both we want to avoid when designing a neural architecture and optimizing an existing one. The scaling strategies for efficiently increasing the size and predictive performance of CNN by the authors of EfficientNet [4], [5], and EfficientDet [4], [6], [5] headed almost in the same direction. They propose scaling the neural architecture in concert with the input resolution. However, contrary to our approach, their proposed scaling still required an expensive grid-search.

This work investigates whether the relationship between input resolution and receptive field can be further exploited as a heuristic for designing and optimizing CNN classifiers. Our primary contribution can be summarized as answers to the following questions:

- Is it possible to predict unproductive subsequences of layers? Answer: Yes, predicting unproductive sequences for simple sequential CNN architectures and architectures with multiple CNN pathways and residual connections before training is possible.
- Since attention mechanisms like SE-Modules [7] effectively provide global context to the feature map, do they change how the inference is distributed? Answer: No, the distribution of the inference process is not affected by the use of simple attention mechanisms. Thus it is still possible to predict unproductive, i.e., unnecessary layers before training.
- Can design decisions be made based on the analysis of the receptive field? Answer: Yes, we demonstrate basic strategies that yield reliable improvements in efficiency and predictive performance .

II. BACKGROUND

This section briefly introduces the essential background knowledge framing this paper. First, analysis techniques for judging the quality of intermediate solutions and the processing within hidden layers are briefly explained and elaborated on pathological inefficiencies. Finally, the receptive field of convolutional layers is discussed and how the receptive field size in sequential and non-sequential architectures are computed.

A. Logistic Regression Probes

For the analysis of trained models, the logistic regression probes (LRP) and the saturation values can be used. For LRP, the input images are replaced with the output of the probed layer l of the CNN, which should be analyzed. Thus the output of the hidden layer is used as the input of the LRP. Since the softmax layer and the probes effectively solve the same task, LRP can judge the quality of the intermediate solutions with

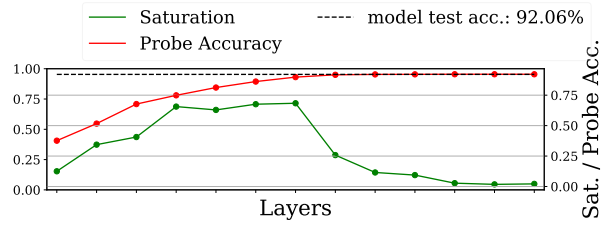


Fig. 2. VGG16 exhibits a *tail pattern* starting from layer Conv8. In the tail, the saturation value is low and the LRP accuracy is stagnating at the same layer. [3]

their validation accuracy. Typically LRP performance increase layer by layer approaching the model’s performance, as shown in Fig. 2). In this paper, the test accuracy of a probe computed on the output of layer l is referred as p_l .

B. Saturation Values and Tail Patterns

Saturation is another technique for expressing the activity of a neural network layer in a single number, proposed by Richter et al. [3]. Saturation s_l is the percentage of eigendirections on the output of layer l required to explain 99% of the variance. Similar to the accuracy of a LRP classifier, this results in a value bound between 0 and 1. Intuitively saturation measures a percentage of how much the output space of a layer is “filled” or “saturated” with the data. A sequence of low saturated layers with $< 50\%$ of the average saturation of all other layers is referred to as *tail pattern*. The *tail pattern* indicates that layers with $< 50\%$ of the average are not contributing qualitatively to the prediction, illustrated as green curve in Fig. 2. The *tail pattern* is also visible when observing the performance of the LRP, plotted as red curve in Fig. 2, which performance stagnate beginning at the same convolution layer.

C. Size of the Receptive Field

The receptive field is the area on an image that influences the output of a convolution operation. For sequential CNNs—no multiple pathways during the forward pass—the receptive field size can be computed analytically. The receptive field r of the l th layer of sequential network structure is referred to as r_l . This work assumes $r_0 = 1$, which is the “receptive field” of the ANN’s input values. For all layers $l > 0$ in the convolutional part of a sequential network the receptive field can be computed with the following formula:

$$r_l = r_{l-1} + ((k_l - 1) \prod_{i=0}^{l-1} s_i) \quad (1)$$

where k_l refers to the kernel size of layer l with potential dilation already accounted for and s_i the stride size of layer i . The receptive field increases with every convolutional layer l with $k_l \neq 1$. Downsampling occurs when $s_l > 1$ and has a multiplicative effect on the growth of r_{l+n} .

The definition mentioned above of receptive field is not feasible for CNNs with a non-sequential structure. An CNN is defined as non-sequential when there is more than one

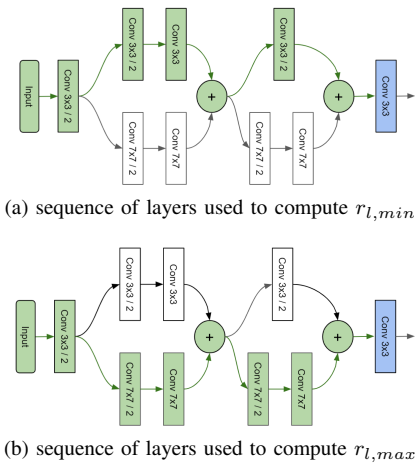


Fig. 3. Sequences of layers used to compute the minimum (a) and the maximum (b) of layer l 's receptive field of a non-sequential architecture are highlighted in green. Sequences of layers used to compute both extrema are highlighted in blue.

sequence of layers leading from the input to the output. Thus, non-sequential CNNs are, e.g., the InceptionV3 [8] due to its parallel layers and ResNet [9]. due to its skip connections

For non-sequential CNN all n possible different receptive field sizes $r_{l_1,min}$ to $r_{l_n,min}$ and $r_{l_1,max}$ to $r_{l_n,max}$ for a certain layer l are computed. The maximum receptive field size of a layer l refers to the largest possible receptive field size $r_{l,max} = \max\{r_{l_1,max}, \dots, r_{l_n,max}\}$, while the minimum size refers to $r_{l,min} = \min\{r_{l_1,min}, \dots, r_{l_n,min}\}$. As Fig. 3 shows, the values for $r_{l,max}$ and $r_{l,min}$ are obtained by computing r_l for the sequences layers with the largest and smallest receptive field leading to l .

III. EXPERIMENTAL SETUPS

This section will discuss the general methodology used for experiments and analysis. If not explicitly mentioned otherwise, all models are trained on the Cifar10 [10] dataset. Since research requires many experiments and the training model as well as LRP are a very resource-intensive process, using Cifar10 as a lightweight dataset is necessary. Remember, Cifar10 is not a trivial task and is commonly used as a proxy problem for larger datasets like ImageNet [1], [2]. The selected CNNs mentioned in paper are primarily chosen because their architectures have certain properties important to investigate experimentally, as a simple sequential structure in the case of VGG16 and skip connections in the case of ResNet18. These architectures were also chosen based on their relatively simple structure that makes them easy to visualize to a broad audience.

1) *Model training*: is conducted for 60 epochs, using stochastic gradient descent (SGD) with a learning rate of 0.1 and a momentum of 0.9 for all evaluated CNN architectures. The learning rate decays every 20 epochs with a decay factor of 0.1. The batch size chosen for this training is 64. Pre-processing further involves channel-wise normalization using μ and σ values taken from original Alexnet paper [11]. During

training, the images are furthermore randomly cropped and horizontally flipped with a 50% probability.

2) *Saturation*: is computed during training of the final epoch on every convolutional and fully connected layer using a δ of 99%, which is the standard configuration recommended by Richter et al. [3].

3) *LRPs*: are trained on the same layers as saturation after the model training. By training the LRPs, this work differs from the procedures of Alain et al. [12] by not global-pooling the feature maps to a single vector in order to avoid artifacts caused by the aggressive downsampling. Based on studies Richter et al. [3], large feature maps to a size of 4×4 pixels are adaptive average pooled, which is a good compromise between computational feasibility and reliability of the test accuracy obtained from the LRPs.

IV. PREDICTING UNPRODUCTIVE LAYERS WITH RECEPTIVE FIELD SIZES

From the results of Richter et al. [3] it is apparent that a mismatch between input resolution and neural architecture will result in sub-sequences of unproductive and therewith unnecessary layers. These unproductive layers are marked by stagnating logistic regression probe performances as well as significantly lower saturation levels compared to the rest of the network cf. *tail pattern* in Fig. 2. The *tail pattern* can be interpreted as a subsequence of layers not contributing to the quality of the network's output. Thus it can be hypothesized that the receptive fields of the individual convolutional layers play a significant role in this observed mismatch between neural architecture and input resolution. One can suspect the role of the receptive fields because it is possible for a layer l to receive input from a convolutional layer $l - 1$ with r_{l-1} bigger than the input resolution i . In this case, no additional context can be added to a feature map position by expanding the receptive field. As a key role in the emergence of unproductive sub-sequences of layers, the inability of such a layer to integrate novel information into a single feature map position is suspected.

In this section we investigate whether it is possible to predict which layers will be unproductive for simple sequential neural architectures. We define a simple sequential architecture as a CNN that can be described as a sequence of convolutional and pooling layers. The VGG-family of networks by [13] are a good example for such architectures, which is the reason why we will make use of these in our initial experiments.

We hypothesize that layers become unproductive if they are unable to integrate novel information into a single feature map position. This is the case when $r_{l-1} > i$, where i is the input resolution. Since the receptive field size grows monotonically in a simple sequential architecture we should be able to define a clear border separating the productive part of the model from the unproductive part based on the condition $r_{l-1} > i$. We refer to the first layer l with $r_{l-1} > i$ as *border layer* b , since it effectively separates the productive from the unproductive part of the model. We test this hypothesis by training VGG11, 13, 16 and 19 on Cifar10 using its native resolution. In all

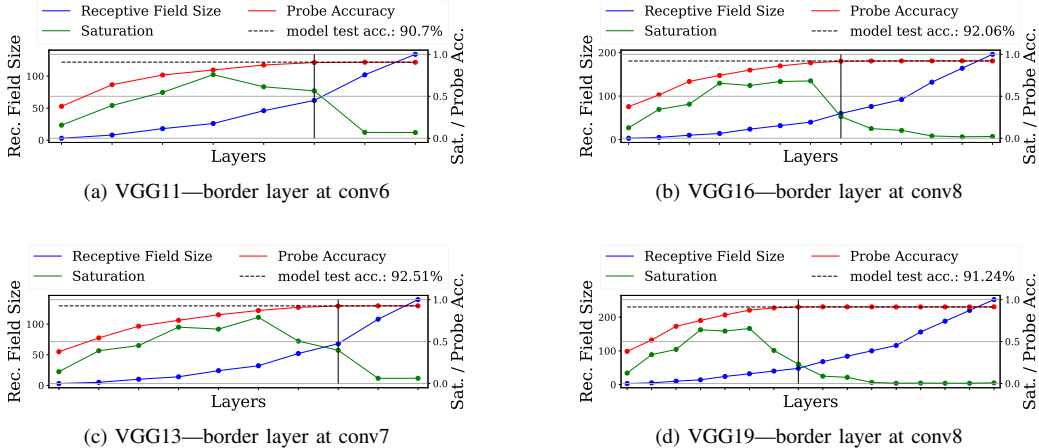


Fig. 4. By analyzing the receptive field, we able to predict the start of the unproductive part of the network. The border layer, marked with a black bar, separates the part of the network that contributes to the quality of the prediction from the part that does not. The border layer is the first layer with a $r_{l-1} > i$, where i is the input resolution.

four cases depicted in Fig. 4 layers before the border layer are highly saturated and improve the probe performance. The layers after the border layer are low saturated and do not improve the probe performance. The observed behavior is also reproducible when training the models on TinyImageNet, while using the same setup otherwise (see Fig. 5).

We show with the VGG-family of networks that this behavior is consistent over different network depths. We also investigate whether changes in the architecture that affect the receptive field produce results consistent with the previous observations. In order to do so, we repeat the Cifar10 experiments using two additional architectures. The first experiment uses a modified ResNet18 [9] with disabled skip connections, making it a sequential architecture. This sequential model differs from VGG-style models in numerous ways. ResNet18 uses BatchNorm [15] and utilizes strided convolutions instead of MaxPooling layers for downsampling. Furthermore ResNet18 features a stem, consisting of two consecutive downsampling layers at the input of the model, which strongly affect the growth of the receptive field size. The second experiment utilizes a modified VGG19 with dilated convolutions, increasing the kernel sizes to 7×7 . From Fig. 6 we can see that the border layer is still separating the solving part from the unproductive part. The observation is thus consistent with previous experiments.

V. THE BORDER LAYER CAN BE PREDICTED USING THE $r_{l,min}$ FOR NON SEQUENTIAL ARCHITECTURES

In this section we investigate whether predicting unproductive sequences of layers is possible when the network structure is non-sequential.

In order to do so, a simple multi-pathway architecture is required that can serve as a "model organism", similar to the VGG-networks in previous experiments. This basic architecture is depicted in Fig. 7. It follows the design conventions regarding downsampling and general structure utilized

in various architectures such as ResNet, VGG, Inception-ResNet, EfficientNet and many other [16], [13], [9], [4]. The architecture has 4 stages consisting of building blocks with similar filter sizes. The first layer in each stage is a downsampling layer that reduces the size of the feature maps by having a stride size of 2. We use two distinct building blocks for two architecture variants. The first, shallow variant uses 2 of the building blocks depicted in Fig. 7 (b) per stage. The building block consists of a 3×3 convolutional path and a 7×7 convolutional path, which are combined again by an element-wise addition. The second, deeper variant uses 4 of the building blocks depicted in Fig. 7 (c). This building block features a different number of layers in each pathway and thus a larger difference between $r_{l,min}$ and $r_{l,max}$. The convolutional layers generally utilize same-padding, batch normalization and ReLU-activation functions, which can be considered standard for many common architectures. We choose element wise addition to unite the pathways, since it does not increase the number of filters like concatenation. This decision avoids the usage of 1×1 convolutions for dimension reduction, which could induce noisy artifact into the analysis. The two distinct pathways with distinct kernel sizes make it easy to compute $r_{l,min}$ and $r_{l,max}$. Another advantage is that these pathways combined contain all layers and only overlap in the first layer. This allows us to analyze the architecture as two sequences of layers, greatly simplifying the visualization in Fig. 8. We choose the layout to observe whether changes to the number of layers and a stronger deviation in the receptive field sizes within a module affect the distribution of the inference process in unexpected ways.

We reuse the same experimental setup from the previous section regarding training and evaluation. However, we visualize the receptive field r_l , saturation s_l and probe performance p_l for the path of the smallest and largest receptive field size as separate sequences. These paths are sequential and only share the first and last layer of the model. We refer to the sequence

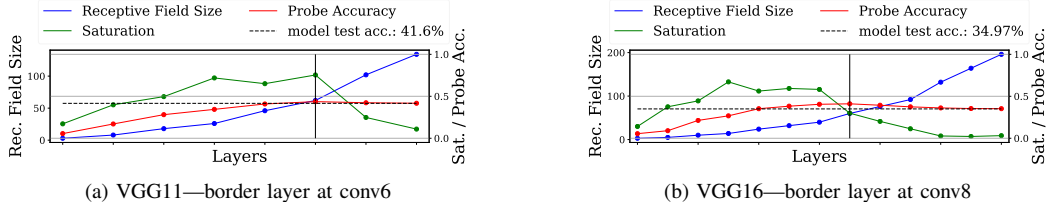


Fig. 5. The prediction by the border layer shown in Fig. 2 holds true for other datasets, as long as the input resolution stays the same. In the depicted case the models are trained on TinyImageNet [14]

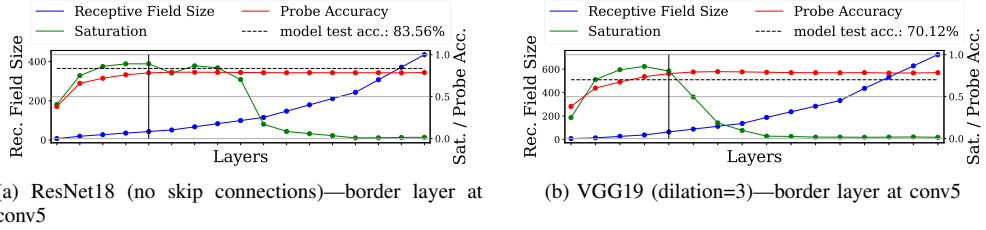


Fig. 6. Predicting unproductive layers with the border layer is also accurate for other architectures. ResNet18 with disabled skip connections (a) uses two initial downsampling layers. The depicted VGG19 variant (b) uses dilated convolutions. Both properties affect the growth of the receptive field differently compared to the models in Fig. 4.

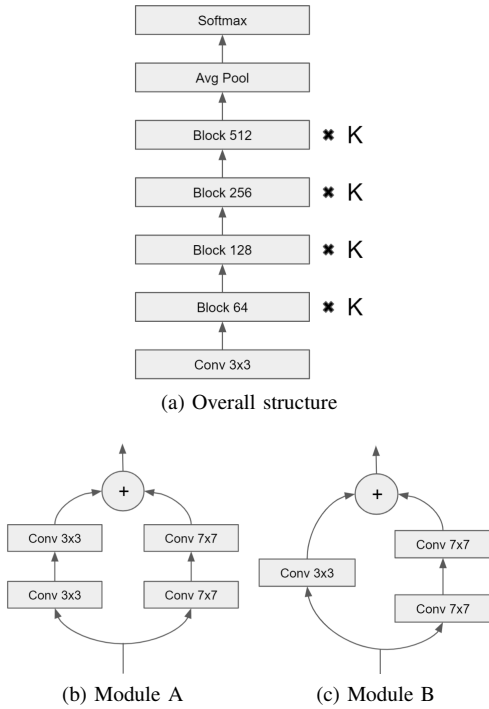


Fig. 7. The architecture used for the experiments in this section. Each stage consists of k blocks and has double the filters of the previous stage. The first layer of each stage is a downsampling layer with a stride size of 2. The building block for the small architecture is depicted in Fig. 7(b), the building block of the deeper architecture is depicted in Fig. 7(c).

of probe performances and layer saturation as $p_{l,min} / p_{l,max}$ and $s_{l,min} / s_{l,max}$ respectively, analog to the designation of the receptive fields in both paths through the network.

From the results in Fig. 8 we can see that in both archi-

tectures the probes of both pathways perform very similar. Interestingly, the border layer b_{max} based on the largest receptive field has no apparent effect on the development of the solution quality. However, the border layer b_{min} of the smallest receptive field exhibits the same behavior that was observed for the border layers of Fig. 2 and 6. This supports the notion that the integration of novel information is critical for the improvement of the solution. However it also shows that the network will not greedily integrate all available information as soon as possible into a single position on the feature map.

VI. RESIDUAL CONNECTIONS ALLOW QUALITATIVE IMPROVEMENTS PAST THE BORDER LAYER

Skip connections are a special case of non-sequential architectures, since they effectively feature pathways that do not expand the size of the receptive field and often contain no layer. Multiple versions of skip connections have been proposed over the years, which generally deviate in the way the pathways are reunited and whether the skip connection itself is parameter-less ([9], [17], [18]). In this work we primarily focus on the residual connection proposed by the authors of [9], which uses an element-wise addition for reuniting the pathways. This skip connection only contains parameters if the residual block is downsampling the feature map with the first layer. We made this decision since it is the most commonly used type of skip connection in popular architectures such as ResNet and its many derivatives like AmoebaNet, MobileNetV2, MobileNetV3, EfficientNet and EfficientNetV2 (only to name a few) [9], [2], [19], [20], [4], [5].

If the receptive field expansion behavior is consistent with the behavior of multi-path architectures discussed in the previous section, b_{min} should predict the unproductive tail of layers.

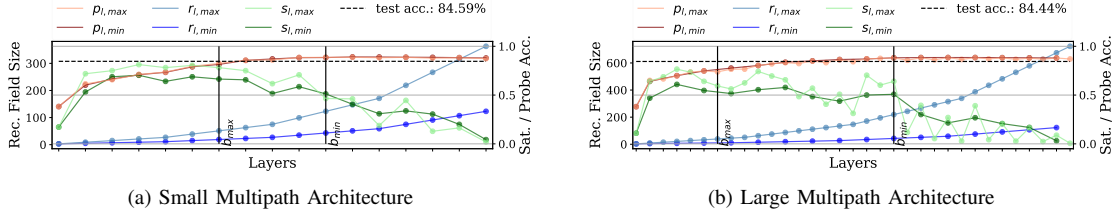


Fig. 8. The border layer b_{min} of the path of the smallest receptive field can predict stagnating layers in both pathways, similar to the border layer in sequential architectures.

We compute $r_{l,min}$ for the convolutional layers and compute the border layer b_{min} based on this sequence of receptive field sizes. From the results in Fig. 9 we can clearly see that this is the case. In both scenarios the qualitative improvement of the predictive performance stops when reaching the border layer. The zick-zack-pattern of the minimal receptive field size originates from the fact that residual connections effectively allow the network to skip all layers except the stem, effectively "resetting" the receptive field size at each residual block. The increasing "amplitude" of this zick-zack pattern in later parts of the network is caused by the additional downsampling layers that increase the growth rate of the receptive field size. There are also additional anomalies present in the probe performances of ResNet18 and ResNet34 in the form of sudden drops of the predictive performance, occurring exclusively after the border layer. We find that these are the result of "skipped" layers, where the model does not utilize layers and "bypasses" them using the skip connection. This phenomenon was first observed by the authors of [12]. Effectively the skipped layers learn a representation of the data that does not carry any information but that does also not cancel out information when added back to the layer's input.

VII. ATTENTION MECHANISMS DO NOT INFLUENCE THE DISTRIBUTION OF THE INFERENCE PROCESS

In this work we consider attention mechanisms, simple layer add-ons that generate dynamical weights based on the input. Squeeze-and-Excitation modules [7] are a filter-wise attention mechanism, since the weighting is applied on each feature map. A spatial attention mechanism instead applies a weight on each feature map position and CBAM [21] is a combination of both. In all cases one or multiple auto-encoder-like structures are condensing the entire stack of feature maps into a set of weights usually with the aid of some global pooling strategy [22]. Therefore the attention mechanism incorporates global information about the image into the feature map via multiplication and therefore changes the information present in each position of the feature map.

Thus our working hypothesis is that attention mechanisms do influence how the inference process is distributed in a convolutional neural network. We test this hypothesis by training two sets of ResNet models. Set A consists of ResNet18 as a reference as well as three versions with different attention mechanism each. These attention mechanisms are:

spatial attention, squeeze-and-excitation-modules and CBAM [7], [21]. We compute saturation and probe performances for all these networks. We thereby omit additional layers added by the aforementioned attention mechanism to make the sequences of probe performances and saturation levels comparable. The remaining setup is the same as in previous experiments conducted on Cifar10. Set B contains the same architectures as set A, but with disabled skip connections. We choose these two sets to also observe whether skip connection have some unexpected interaction with attention mechanisms.

In both cases our working hypothesis can be rejected, judging from the results in Fig. 10. While the accuracy varies depending on the used attention mechanism, the patterns in the sequence of probe performances and saturation levels do not change significantly, regarding unproductive and productive sequences of layers. From this we can conclude that attention mechanisms primarily change the way a layer extracts the features. However, attention apparently does not change how the overall inference is distributed. This also means that the results from previous experiments regarding the role of b_{min} for predicting unproductive layers is not influenced by the use of any attention mechanism tested in this work.

VIII. IMPLICATIONS ON NEURAL ARCHITECTURE DESIGN

Since we are able to predict unproductive sequences of layers given only the architecture and input resolution, we can leverage this knowledge to improve architectures. The biggest advantage of this is that both properties are known before the start of training and thus allow for a very efficient design process, since the architecture can be optimized without requiring multiple training steps for comparative evaluation.

We exemplify, by employing a very simple optimization strategy. VGG11, 13, 16, 19, ResNet18, ResNet34 as well as the multi-path architectures used in section in section V, abbreviated as MPNet18 and 36, are trained on Cifar10. We then train truncated variants of these architectures where all layers of the tail are replaced by a simple classifier consisting of a global average pooling layer followed by a softmax layer. This can be seen as the simplest possible change to the architecture that removes the tail pattern. We train all models 10 times and average the test accuracy to mitigate the random fluctuations in the predictive performance. We further compute the number of parameters and flops required for a forward pass of a single image. The results are visualized in Fig. 11.

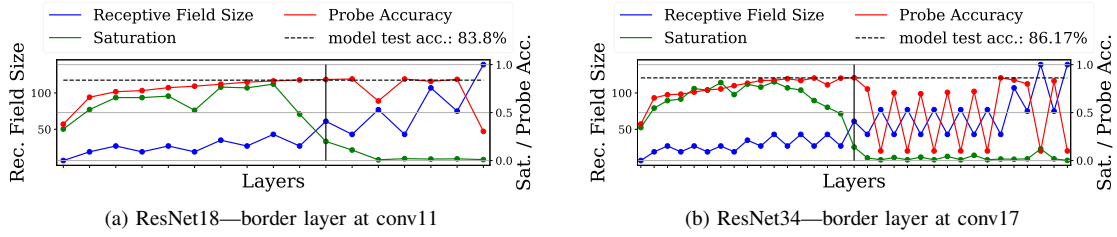


Fig. 9. The border layer computed from the smallest receptive field size b_{min} can predict unproductive layers for ResNets. The skip connections allow information based on smaller receptive field sizes to skip layers, resulting in a later border layer b_{min} compared to the same network with disabled skip connections. This allows networks with skip connections to involve more layers in the inference process than it would be possible compared to a simple sequential architecture with a similar layout. For an example compare Fig. 6 (a) with Fig. 9 (a).

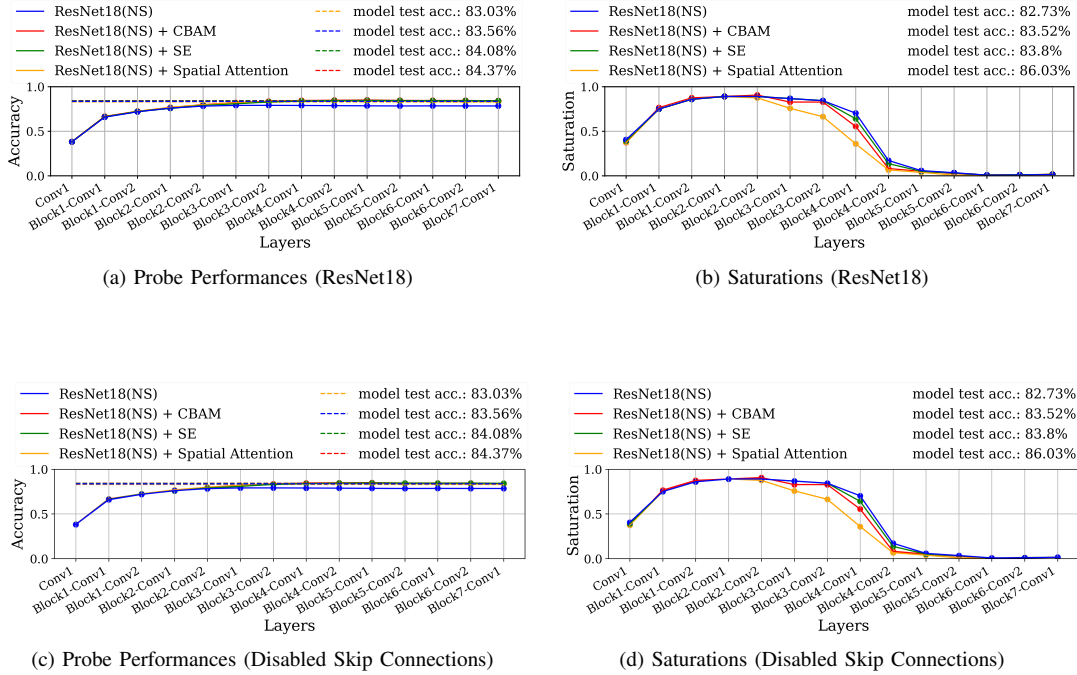


Fig. 10. Spatial Attention, Filter Wise Attention (SE) as well as a combination of both does neither change the probe performances nor the accuracy in any significant manner, indicating that they aid the feature extraction for the receptive field size present, but do not change the size of features extracted.

The performance of the truncated models also improves in all tested scenarios. Since the flops and parameters are reduced by the removal of layers, all tested architectures become more efficient compared to their un-truncated counterparts trained on the same setup.

The demonstrated technique can be considered crude and is not necessarily the most effective way of improving the predictive performance. Another possibility to remove unproductive layers is to influence the growth rate of the receptive field in the neural architecture. This can be done by adding, removing or re-positioning pooling layers in the network. For instance by removing the first two downsampling layers (stem) in ResNet18 and ResNet34 the growth of the receptive fields in the entire network is reduced by a factor of 4. Removing the stem in ResNet34 improves the performance from

82.76% to 92.21%, for ResNet18 the improved performance is 91.95 % from the previous 84.61%, removing the tail in the process. However, while this is an improvement on predictive performance and parameter efficiency, we reduce computational efficiency in the process. The removal of the stem will increase the flops per image, since the effective size of the feature map is increased in every layer. This is the case because the removal of a downsampling layer not only reduces the growth of the receptive field for consecutive layers but also increases the size of the feature maps. This in turn increases the computations required to process these layers, since more positions of convolutional kernel need to be evaluated. In case of ResNet34 the computations per forward pass increase from 0.76 GFLOPS to 1.16 GFLOPS, for ResNet18 the computations increase from 0.04 GFLOPS to

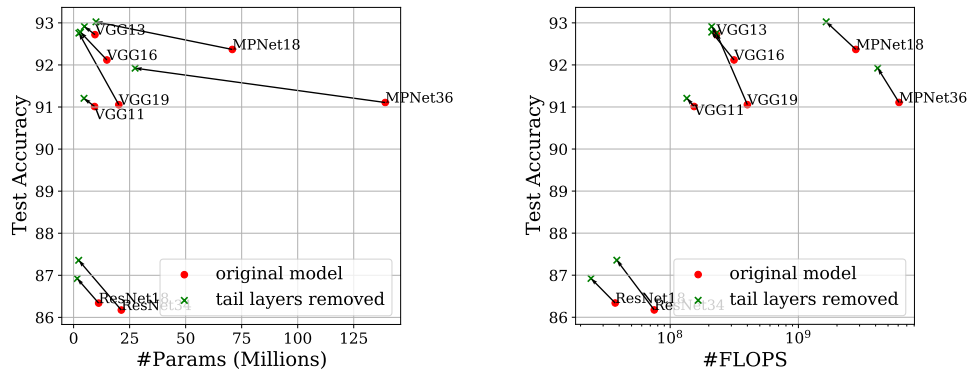


Fig. 11. A simple exemplary modification based on receptive field analysis is removing the tail layers from the architecture. Removing these layers improves the efficiency by improving the performance as well as reducing the number of parameters and computations required.

0.56 GFLOPS. This change to the architecture demonstrates that there is no singular optimal path to a well performing convolutional neural architecture. This is also the main reason why we do not provide an optimization algorithm.. Instead changes to the architecture often are a trade-off between predictive performance, parameter-efficiency and computational efficiency. The best decision for a given scenario depends on the scenario itself and the requirements of the task regarding the model. However, by analyzing the receptive field, the trade-off decision can be made more quickly and in a more informed, intentional manner.

IX. CONCLUSION

While often building ever deeper and more powerful neural architectures is crucial for pushing the state of the art, we think that also designing lightweight and efficient neural architectures is crucial for opening deep learning to a broader range of applications with limited resources. The results presented in this work allow users to detect inefficiencies in convolutional neural architectures before training the model and allow for improving these architectures deterministically and reliably. By exploring the properties of multi-path architectures and architectures with residual connection and attention mechanisms, we have covered a broad range of common architectural components used in modern neural networks and incorporated them into our design guidelines, allowing for degrees of freedom in the design process that very directly allow the data scientist to make decision in favor of either computational power, predictive performance and parameter efficiency. Making model more parameter efficient could further lead to more models that need smaller amounts of data. This could further increase the sustainability and viability of deep learning solutions, enabling a even broader field of potential applications.

REFERENCES

- [1] M. Tan, B. Chen, R. Pang, V. Vasudevan, and Q. V. Le, "Mnasnet: Platform-aware neural architecture search for mobile," *CoRR*, vol. abs/1807.11626, 2018. [Online]. Available: <http://arxiv.org/abs/1807.11626>
- [2] E. Real, A. Aggarwal, Y. Huang, and Q. V. Le, "Regularized evolution for image classifier architecture search," 2019.
- [3] J. Shenk, M. L. Richter, W. Byttner, A. Arpteg, and M. Huss, "Feature space saturation during training," 2020.
- [4] M. Tan and Q. Le, "EfficientNet: Rethinking model scaling for convolutional neural networks," in *Proceedings of the 36th International Conference on Machine Learning*, ser. Proceedings of Machine Learning Research, K. Chaudhuri and R. Salakhutdinov, Eds., vol. 97. PMLR, 09–15 Jun 2019, pp. 6105–6114. [Online]. Available: <http://proceedings.mlr.press/v97/tan19a.html>
- [5] M. Tan and Q. V. Le, "Efficientnetv2: Smaller models and faster training," 2021.
- [6] M. Tan, R. Pang, and Q. V. Le, "Efficientdet: Scalable and efficient object detection," 2020.
- [7] F. N. Iandola, S. Han, M. W. Moskewicz, K. Ashraf, W. J. Dally, and K. Keutzer, "Squeezenet: Alexnet-level accuracy with 50x fewer parameters and 10.5mb model size," 2016.
- [8] C. Szegedy, V. Vanhoucke, S. Ioffe, J. Shlens, and Z. Wojna, "Rethinking the inception architecture for computer vision," *CoRR*, vol. abs/1512.00567, 2015. [Online]. Available: <http://arxiv.org/abs/1512.00567>
- [9] K. He, X. Zhang, S. Ren, and J. Sun, "Deep residual learning for image recognition," *CoRR*, vol. abs/1512.03385, 2015. [Online]. Available: <http://arxiv.org/abs/1512.03385>
- [10] A. Krizhevsky, V. Nair, and G. Hinton, "Cifar-10 (canadian institute for advanced research)." [Online]. Available: <http://www.cs.toronto.edu/~kriz/cifar.html>
- [11] A. Krizhevsky, I. Sutskever, and G. E. Hinton, "Imagenet classification with deep convolutional neural networks," in *Advances in Neural Information Processing Systems*, F. Pereira, C. J. C. Burges, L. Bottou, and K. Q. Weinberger, Eds., vol. 25. Curran Associates, Inc., 2012.
- [12] G. Alain and Y. Bengio, "Understanding intermediate layers using linear classifier probes," 2018.
- [13] K. Simonyan and A. Zisserman, "Very deep convolutional networks for large-scale image recognition," 2015.
- [14] Y. Le and X. Yang, "Tiny ImageNet Visual Recognition Challenge," 2015.
- [15] S. Ioffe and C. Szegedy, "Batch normalization: Accelerating deep network training by reducing internal covariate shift," 2015.
- [16] C. Szegedy, S. Ioffe, V. Vanhoucke, and A. Alemi, "Inception-v4, inception-resnet and the impact of residual connections on learning," 2016.
- [17] R. K. Srivastava, K. Greff, and J. Schmidhuber, "Highway networks," 2015.
- [18] G. Huang, Z. Liu, and K. Q. Weinberger, "Densely connected convolutional networks," *CoRR*, vol. abs/1608.06993, 2016. [Online]. Available: <http://arxiv.org/abs/1608.06993>
- [19] M. Sandler, A. Howard, M. Zhu, A. Zhmoginov, and L.-C. Chen, "Mobilenetv2: Inverted residuals and linear bottlenecks," 2019.

- [20] A. Howard, M. Sandler, G. Chu, L.-C. Chen, B. Chen, M. Tan, W. Wang, Y. Zhu, R. Pang, V. Vasudevan, Q. V. Le, and H. Adam, "Searching for mobilenetv3," 2019.
- [21] S. Woo, J. Park, J.-Y. Lee, and I. S. Kweon, "Cbam: Convolutional block attention module," in *Proceedings of the European Conference on Computer Vision (ECCV)*, September 2018.
- [22] M. Lin, Q. Chen, and S. Yan, "Network in network," 2014.